

Supplementary Information**Supplementary Figure 1. Clathrin fragments containing the N-terminal domain can bind MTs *in vitro*, but only in presence of mitotic extract.**

(A) Western blot of a typical MT spin-down experiment. In the absence of mitotic extract, MBP-tagged clathrin fragments do not show MT-dependent co-pelleting. When the reaction was supplemented with mitotic extract, both MBP-CHC(1-579)*-His and MBP-CHC(1-1074)-His, but not MBP-His, co-pelleted with MTs. (B) Coomassie blue-stained 12 % SDS-PAGE gel of control MT spin-down reactions to show MT-dependent co-pelleting of MAP fraction but not BSA.

Supplementary Figure 2. Quantification of RNAi efficiency.

(A) HeLa and (B) HEK293 cells were transfected with pBrain plasmids that express a fluorescent reporter together with shRNA targeting either TACC3, ch-TOG or CHC, as indicated. The time period post-transfection was 3 days for TACC3, ch-TOG and CHC in HEK293, 5 days for CHC and 2 days for TACC3 and ch-TOG in HeLa. Cells were then fixed and stained with antibodies to assess depletion of endogenous TACC3, ch-TOG or CHC. Representative fluorescence micrographs are shown (Open arrows = pBrain transfected cells, closed arrows = untransfected cells). Scale bars, 20 μ m. The level of endogenous protein remaining in transfected cells was quantified and compared to control pBrain transfected cells. Bars are mean \pm s.e.m. ***, $p < 0.001$. $n_{\text{cell}} = 26-94$ for HeLa, $n_{\text{cell}} = 13-26$ for HEK293. (C) Western blots of lysates of HEK293 cells transfected with control, CHC or TACC3 pBrain to assess depletion of endogenous protein. (D) Representative micrographs of the cells used for these lysates, with overall transfection efficiency indicated alongside. Due to relatively low transfection efficiencies, the quantification of immunofluorescence data is easier to interpret than western blotting.

Supplementary Figure 3. Effect of expression of GFP-TACC3(S558A) on TACC3 localisation at the mitotic spindle.

(A) Representative confocal micrographs of mitotic cells expressing GFP, GFP-TACC3 or GFP-TACC3(S558A) that were fixed and stained with an anti-TACC3 antibody. Scale bar, 10 μm . (B) Quantification of TACC3 immunofluorescence at the spindle. Bars are mean \pm s.e.m. *, $p < 0.05$.

Supplementary Figure 4. Multi-peak analysis of inter-MT bridges.

Bridge length histograms with a 1 nm resolution were generated for each condition from all bridge measurements. Multi-peak fits were carried out as described in the Methods. We assumed that the populations would follow a Gaussian distribution. Individual Gaussians are shown below and the residuals of the fit are shown above the histogram with the multi-peak fit shown in blue. Analysis of the clathrin experiments (A) and TACC3 experiments (B) are shown.

Supplementary Figure 5. Effect of depletion of ch-TOG on mitotic spindle morphology.

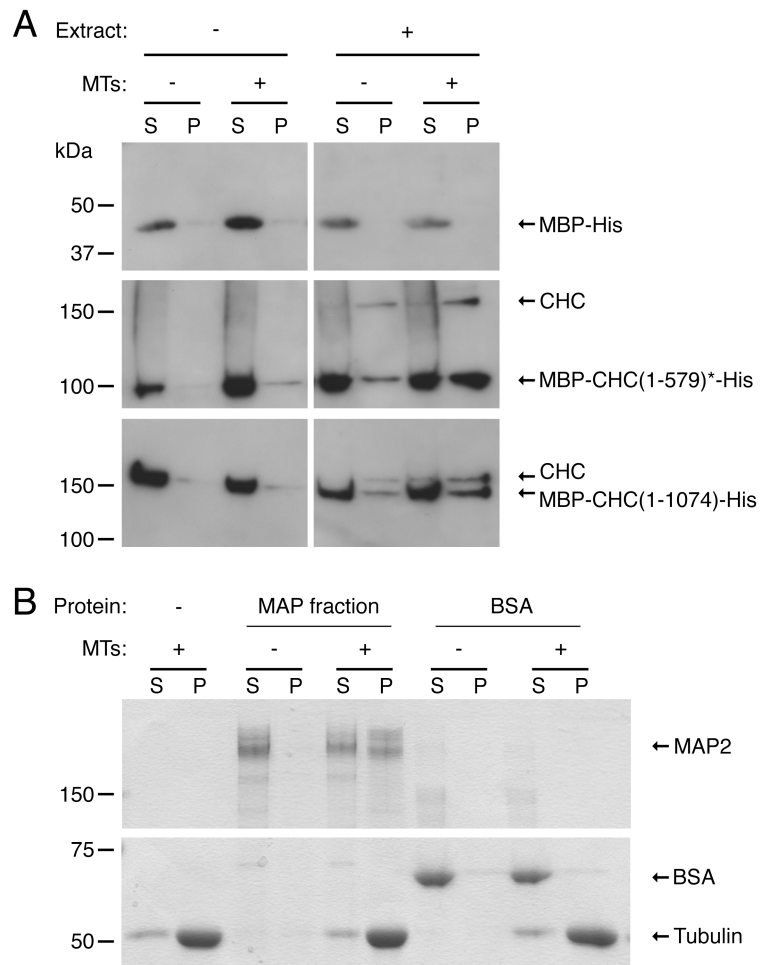
Four cells were studied using correlative light electron microscopy. Cell 1 is untransfected (internal control) and cells 2 - 4 show a progressive range of aberrant mitotic phenotypes as a consequence of ch-TOG depletion using RNAi. (A) Fluorescence micrograph of a field containing four cells that was processed for EM (Left, DNA; Right, GFP). (B) Electron micrographs. Bi) Correlative overviews of cells identified in A. In Bii, zoomed views of an area adjacent to the chromosomes that were boxed in Bi, are shown. In Biii, high magnifications of the boxed areas from Bii are shown. Biii (inset) shows zoomed views of areas in Biii. Cell #1 has a normal K-fibre that can be visualised and analysed normally. Whereas the K-fibres in cells #2-4 were not parallel to the section and could not be quantified. The zoomed areas in Biii (inset) show MTs that are orthogonal to the longitudinal axis of the spindle. Scale bar, 10 μm (A), 4 μm (Bi), 1 μm (Bii), 100 nm (Biii).

Supplementary Figure 6. Model for TACC3/ch-TOG/clathrin inter-MT bridge formation

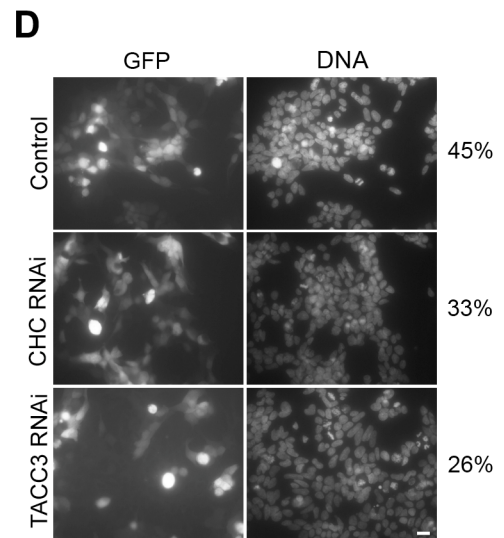
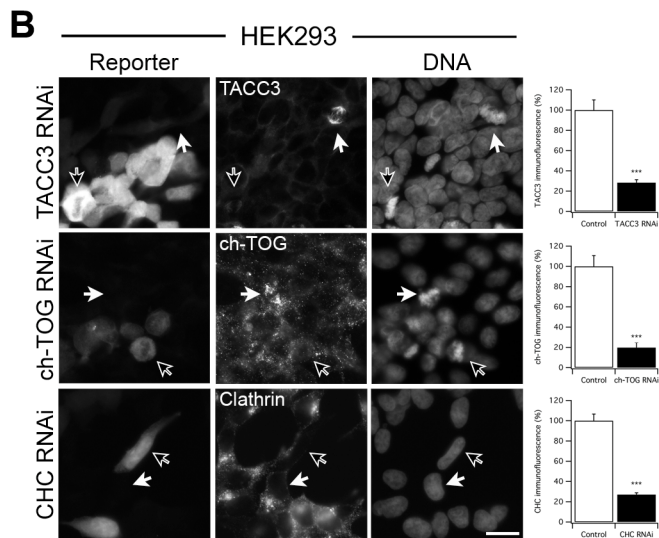
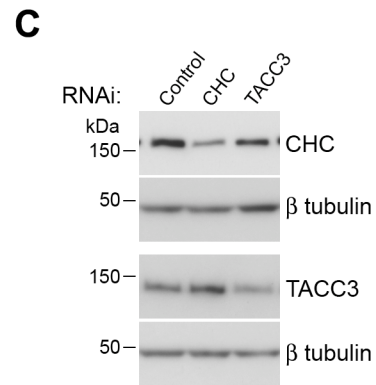
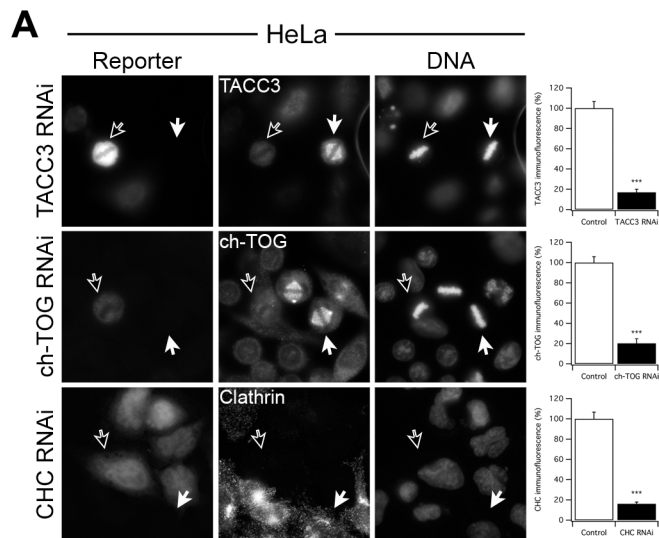
Schematic diagram to show the order of recruitment of TACC3/ch-TOG/clathrin complex components and our proposed mechanism for accumulation of the complex on MTs. 1. Recruitment of TACC3 and ch-TOG to MTs: TACC3 is the primary determinant for binding to MTs, a process regulated by Aurora-A kinase-mediated phosphorylation on Ser558. TACC3 recruits ch-TOG to MTs. 2. Clathrin recruitment: clathrin binds to TACC3 or TACC3/ch-TOG sub-complexes on MTs. 3. Complex accumulation: clathrin binds more than one TACC3 or TACC3/ch-TOG subcomplex on adjacent MTs, locking the complex and causing accumulation. Clathrin therefore bridges between adjacent parallel MTs. The dimensions of clathrin (Heuser & Kirchhausen, 1985) and MTs (Nogales et al, 1999) are approximately to scale.

References

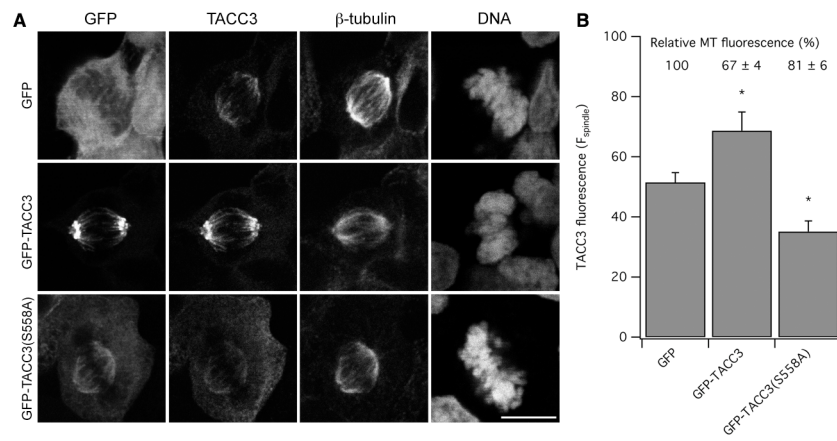
- Heuser J, Kirchhausen T (1985) Deep-etch views of clathrin assemblies. *J Ultrastruct Res* **92**: 1-27
- Nogales E, Whittaker M, Milligan RA, Downing KH (1999) High-resolution model of the microtubule. *Cell* **96**: 79-88



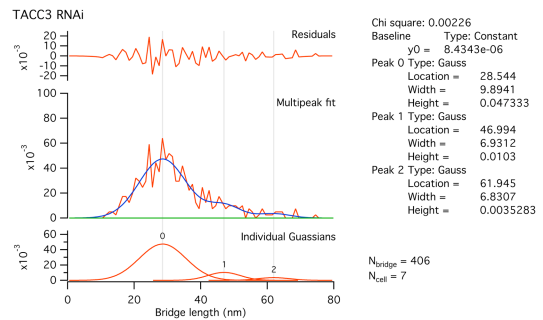
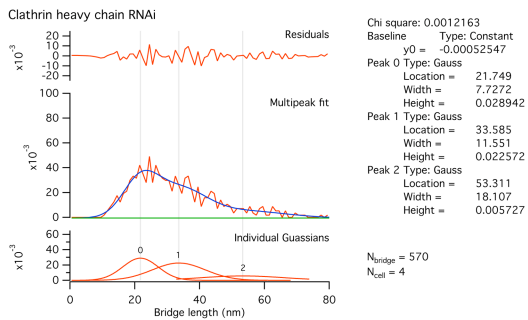
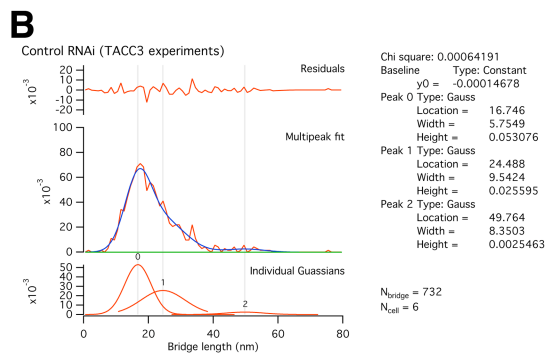
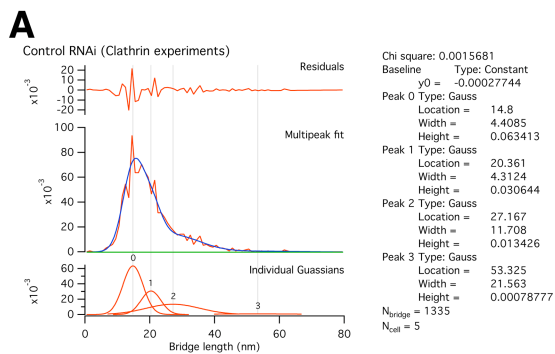
Supplementary Figure 1



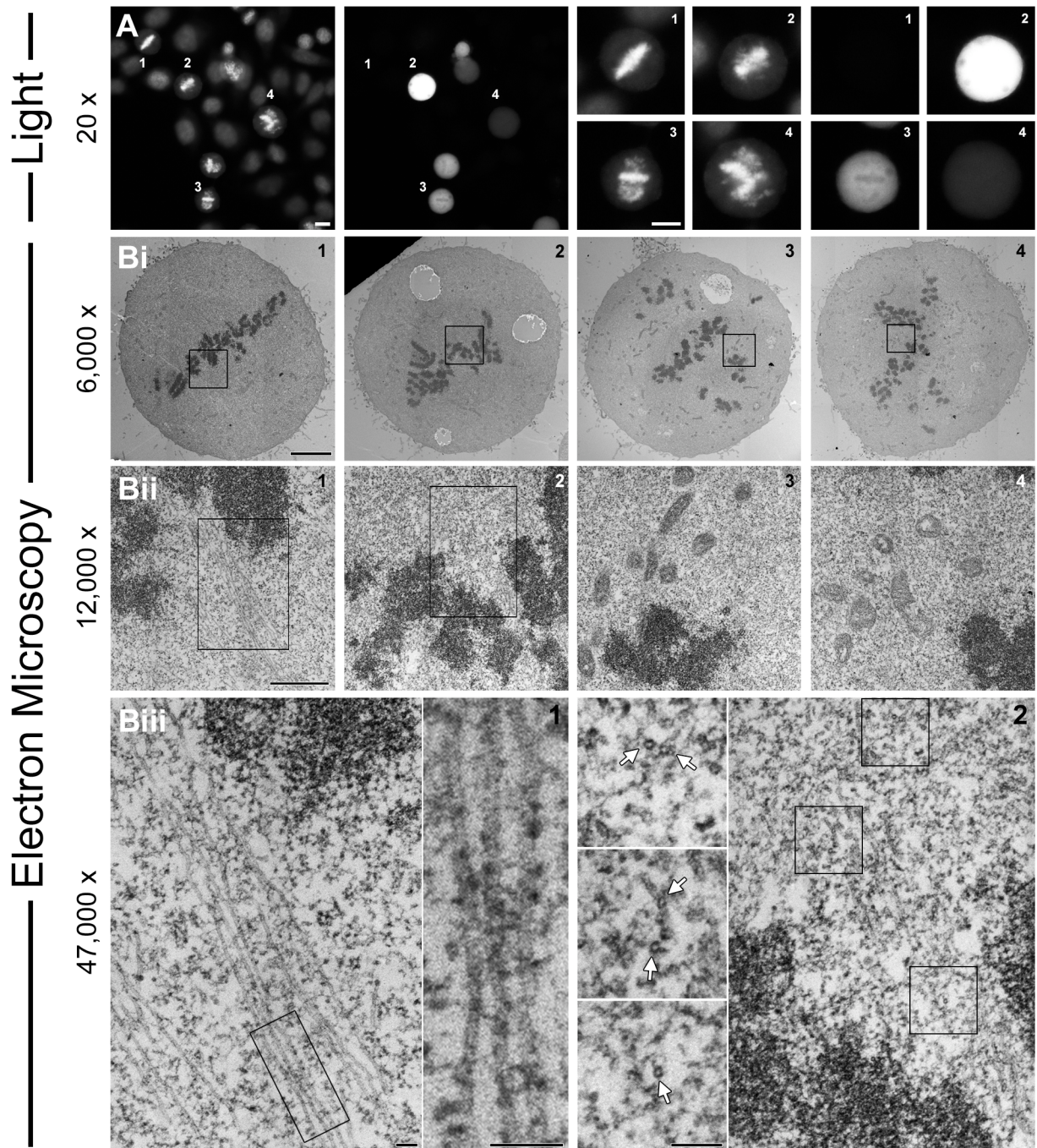
Supplementary Figure 2



Supplementary Figure 3



Supplementary Figure 4



Supplementary Figure 5

